CLINICAL GENETICS An International Journal of Genetics, Molecular and Personalized Medicine

Clin Genet 2011: 80: 293–296
Printed in Singapore. All rights reserved

CLINICAL GENETICS
doi: 10.1111/j.1399-0004.2011.01644.x

Letter to the Editor

A novel homozygous mutation of *DARS2* may cause a severe LBSL variant

To the Editor:

Leukoencephalopathy with brain stem and spinal cord involvement, and lactate elevation (LBSL, MIM #611105) is an autosomal recessive disorder with an early childhood-to-adolescence onset. In 2003, van der Knaap et al. originally described LBSL, which is characterized by slowly progressive pyramidal, cerebellar, and dorsal column dysfunction with increased white matter lactate levels in magnetic resonance (MR) spectroscopy (1). Since the first discovery that LBSL is caused by mutations of the *DARS2* gene-encoding mitochondrial aspartyl-tRNA synthetase (MtAspRS) (2), *DARS2* mutations have been found in all the patients described (2–5), but none of them showed a homozygous mutation (all are compound heterozygotes), suggesting that the activity of mutant MtAspRS homodimers may be incompatible with human life (2, 5). Here, we describe, for the first time, a consanguineous family with a homozygous *DARS2* mutation.

Materials and methods

We analyzed a consanguineous family including three affected children diagnosed with leukoencephalopathy (Fig. 1a and Table 1). The proband (II-2) developed truncal ataxic gait at 3 years old. Her affected sister (II-3) and brother (II-4) also showed truncal ataxia at 6 and 11 months, respectively. All cases were presented with horizontal nystagmus, slurring speech, ataxic gait, muscle tonus abnormality, hypo- or hyperreflexia, and tremor as well as mental retardation. II-2 at age 21 years could slowly speak one or two words. Peripheral muscles atrophy, weakness and joints contractures in extremities, loss of deep tendons reflex and disturbed deep sensation were noted. II-3 and II-4 died of pneumonia at age 8 years and respiratory failure at age 2 years, respectively. Although there were differences in MR imaging characteristics from classical LBSL, there were also striking similarities. In our patients, the involvement of the cerebral and cerebellar white matter was more diffused and severe than in classical LBSL, but the affected brain stem and spinal cord tracts were the same (Fig. 1b and Table 1).

Linkage analysis and direct sequencing of *DARS2* were performed as previously reported (6). Immunoblotting was carried out using antihuman DARS2 antibody (ab69336, Abcam, Cambridge, UK) and anti-cytochrome *c* oxidase (COX) IV antibody (ab16056, Abcam).

Results

Homozygosity mapping of this consanguineous family revealed the largest 8.5 Mb homozygous region at chromosome 1q25.1 with the maximum LOD score of 1.329. Five additional microsatellite markers showed the consistent result (Fig. 1a). Within this region, *DARS2* gene was highlighted as the primary target as it was causative for the LBSL. We found that all affected children possessed homozygous, and parents and an unaffected sib had the heterozygous intronic change at 22 base pairs upstream of exon 3 (c.228-22T>A), respectively. This change was not observed in 395 controls. We examined its mutational effect by reverse transcriptase-polymerase chain reaction (RT-PCR) using mRNA of lymphoblastoid cell lines (LCLs) derived from the proband, her father (a carrier) and a normal control. A shorter PCR fragment which lacked the entire exon 3 was confirmed by sequencing (Fig. 1c,d). Furthermore, wild-type *DARS2* mRNA and MtAspRS protein were significantly decreased in proband's LCL (Fig. 1e,f). Other genes within the 1q25.1 region have not been checked.

Discussion

We found a novel homozygous mutation of *DARS2* in a diffuse leukoencephalopathy, which may be an LBSL variant. This change resulted in the decrease of normal protein level and may have contributed to this disease. Two possibilities for the increased severity are considered: (i) a

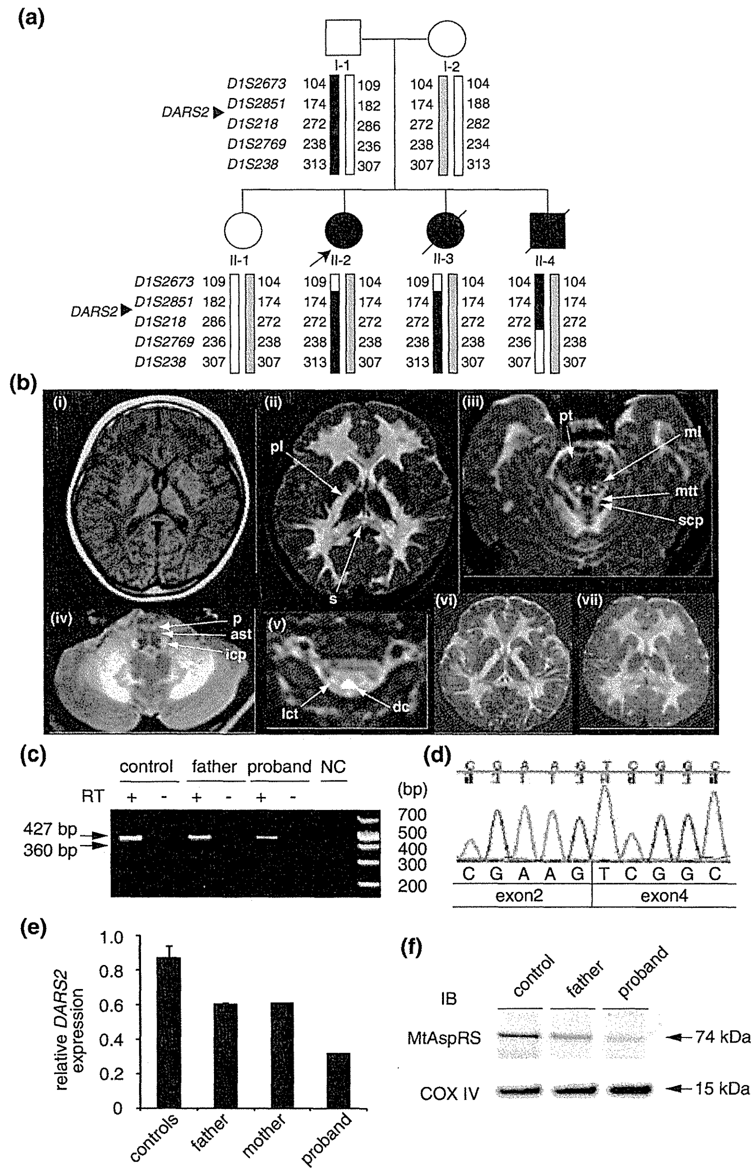

Fig. 1. Identification of a homozygous *DARS2* mutation causing abnormal splicing. (**a**) Haplotype analysis of the family. The black and gray bars represent disease alleles. The *DARS2* gene is located in between *D1S2851* and *D1S218*. (**b**) Magnetic resonance (MR) images of central nervous system in the proband (II-2) at 5 years (i–v), II-3 at 5 years (vi) and II-4 at 1 year and 4 months of age (vii). T_1-weighted (i) and T_2-weighted (T_2) (ii) images of cerebrum. The cerebral white matter was diffusely and severely affected, while the cerebral white matter involvement is less severe and more limited in extent in leukoencephalopathy with brain stem and spinal cord involvement, and lactate elevation with sparing of the U-fibers. Inhomogeneous signal abnormalities were observed in the posterior limb (pl) of the internal capsule and the splenium (s) of the corpus callosum. (iii) T_2 image at the level of the pons. The abnormal high-intensity signals were observed in pyramidal tracts (pt), medial lemniscus (ml), mesencephalic trigeminal tracts (mtt) and superior cerebellar peduncles (scp). (iv) T_2 image at the level of medulla. The pyramids (p), anterior spinocerebellar tracts (ast) and inferior cerebellar peduncles (icp) were affected. (v) T_2 image at the level of the cervical spinal cord. The dorsal columns (dc) and lateral corticospinal tracts (lct) showed abnormal signals. II-3 (vi) and II-4 (vii) showed the similar MR images as the proband. (**c**) RT-PCR using cDNA extracted from LCLs of a normal control, father and the proband. A shorter fragment (360 bp) in addition to a normal product (427 bp) was seen in father and the proband. (**d**) Electropherogram of the shorter fragment showing skipping of exon 3. (**e**) Relative expression of wild-type *DARS2* mRNA compared to β-actin mRNA in LCLs were determined by quantitative real-time RT-PCR using TaqMan Gene Expression Assays (Applied Biosystems, Bedford, MA). The relative *DARS2* expression was analyzed using TaqMan Probe (Applied Biosystems, Hs01016215_m1 for *DARS2* and 4326135E for β-actin as a control). Levels are shown for three controls, parents and the proband based on the calibration curve method using an independent control. Average of duplicated experiments is shown as black bars with the standard error of means. The significant decreased expression of *DARS2* mRNA in the proband was recognized compared to that in three controls ($p < 0.001$, one-way analysis of variance with Bonferroni's multiple comparison test). (**f**) Mitochondrial aspartyl-tRNA synthetase (MtAspRS) protein is expressed in normal control and father as a carrier (fainter), but only weakly recognized in the proband. Cyclooxygenase IV was used as a loading control for the mitochondrial fraction.

Table 1. MRI criteria for LBSL and clinical features of patients

Diagnostic criteria	Case 1	Case 2	Case 3
Major criteria			
Signal abnormalities in			
1. the cerebral white matter, either inhomogeneous and spotty or homogeneous and confluent, sparing the U-fibers	±[a]	±[a]	±[a]
2. the dorsal columns and lateral corticospinal tracts of the spinal cord. (visualization of such abnormalities in the cervical spinal cord suffices)	+	n.e.[b]	n.e.
3. the pyramids of the medulla oblongata	+	+	+
Supportive criteria			
Signal abnormalities in			
1. the splenium of the corpus callosum	+	+	+
2. the posterior limb of the internal capsule	+	+	+
3. the medial lemniscus in the brain stem	+	+	+
4. the superior cerebellar peduncles	+	+	+
5. the inferior cerebellar peduncles	+	n.e.	n.e.
6. the intraparenchymal part of the trigeminal nerve	−	n.e.	n.e.
7. the mesencephalic trigeminal tracts	+	n.e.	n.e.
8. the anterior spinocerebellar tracts in the medulla	+	n.e.	n.e.
9. the cerebellar white matter with subcortical preponderance	−	−	−
Elevated lactate of abnormal cerebral white matter (MRS)	+	Not performed	+

LBSL, leukoencephalopathy with brain stem and spinal cord involvement, and lactate elevation; MRI, magnetic resonance imaging; MRS, magnetic resonance spectroscopy.
[a]Homogeneous and confluent abnormal high intensity was observed, but sparing the U-fibers was unclear because of the strenuous pathological change in the white matter.
[b]n.e., not evaluated as MRI images were unavailable.

(unidentified) modifier effect in the family and (ii) this particular homozygous mutation caused the severe variant because of the substantially decreased normal protein level, although it is not full proof.

Interestingly, affected allele frequency varies, depending on the ethnicity. For example, *DARS2* mutations are the most common causes of childhood onset leukoencephalopathy in Finland, because of high carrier frequency (1:95 for the c.228-20_21delTTinsC and 1:380 for the c.492+2T>C) (4). Thus, further analysis of the *DARS2* gene in LBSL as well as childhood-to-adult onset leukoencephalopathy of unknown cause in different populations would lead us to fully understand phenotypes of the *DARS2* abnormalities.

Acknowledgements

We thank all the patients and their families for participating in this work. We also thank Ms. Y. Yamashita for her technical assistance. This work was supported by Research Grants from the Ministry of Health, Labour and Welfare (N. M., H. S., and N. M.), the Japan Science and Technology Agency (N. M.), Grant-in-Aid for Scientific Research from Japan Society for the Promotion of Science (N. M.), Grant-in-Aid for Young Scientist from Japan Society for the Promotion of Science (N. M. and H. S.), Grant for 2010 Strategic Research Promotion of Yokohama City University (N. M.), Research Grants from the Japan Epilepsy Research Foundation (H. S.), and Research Grant from Naito Foundation (N. M.), the Takeda Science Foundation (N. M. and N. M.), the Yokohama Foundation for Advancement of Medical Science (N. M.) , and the Hayashi Memorial Foundation for Female Natural Scientists (N. M.).

N Miyake[a]
S Yamashita[b]
K Kurosawa[c]
S Miyatake[a]
Y Tsurusaki[a]
H Doi[a]
H Saitsu[a]
N Matsumoto[a]
[a]Department of Human Genetics, Yokohama City University Graduate School of Medicine, Yokohama, Japan,
[b]Division of Child Neurology, and
[c]Division of Medical Genetics, Kanagawa Children's Medical Center, Yokohama, Japan

References

1. van der Knaap MS, van der Voorn P, Barkhof F et al. A new leukoencephalopathy with brainstem and spinal cord involvement and high lactate. Ann Neurol 2003: 53: 252–258.
2. Scheper GC, van der Klok T, van Andel RJ et al. Mitochondrial aspartyl-tRNA synthetase deficiency causes leukoencephalopathy with brain stem and spinal cord involvement and lactate elevation. Nat Genet 2007: 39: 534–539.
3. Uluc K, Baskan O, Yildirim KA et al. Leukoencephalopathy with brain stem and spinal cord involvement and high lactate:

a genetically proven case with distinct MRI findings. J Neurol Sci 2008: 273: 118–122.
4. Isohanni P, Linnankivi T, Buzkova J et al. *DARS2* mutations in mitochondrial leucoencephalopathy and multiple sclerosis. J Med Genet 2010: 47: 66–70.
5. Lin J, Faria EC, Da Rocha AJ et al. Leukoencephalopathy with brainstem and spinal cord involvement and normal lactate: a new mutation in the *DARS2* gene. J Child Neurol 2010: 25: 1425–1428.
6. Miyake N, Kosho T, Mizumoto S et al. Loss-of-function mutations of *CHST14* in a new type of Ehlers-Danlos syndrome. Hum Mutat 2010: 31: 966–974.

Correspondence:
Noriko Miyake, MD, PhD
Department of Human Genetics
Yokohama City University Graduate School of Medicine
3-9 Fukuura
Kanazawa-ku
236-0004 Yokohama
Japan
Tel.: +81 45 787 2606
Fax: +81 45 786 5219
e-mail: nmiyake@yokohama-cu.ac.jp

CLINICAL REPORT

AMERICAN JOURNAL OF medical genetics PART A

Early Infantile Epileptic Encephalopathy Associated With the Disrupted Gene Encoding Slit-Robo Rho GTPase Activating Protein 2 (*SRGAP2*)

Hirotomo Saitsu,[1*] Hitoshi Osaka,[2] Shirou Sugiyama,[2] Kenji Kurosawa,[3] Takeshi Mizuguchi,[1] Kiyomi Nishiyama,[1] Akira Nishimura,[1] Yoshinori Tsurusaki,[1] Hiroshi Doi,[1] Noriko Miyake,[1] Naoki Harada,[4] Mitsuhiro Kato,[5] and Naomichi Matsumoto[1]

[1]Department of Human Genetics, Graduate School of Medicine, Yokohama City University, Kanazawa-ku, Yokohama, Japan

[2]Division of Neurology, Clinical Research Institute, Kanagawa Children's Medical Center, Minami-ku, Yokohama, Japan

[3]Division of Medical Genetics, Clinical Research Institute, Kanagawa Children's Medical Center, Minami-ku, Yokohama, Japan

[4]Cytogenetic Testing Group B, Advanced Medical Science Research Center, Mitsubishi Chemical Medience Corporation, Nagasaki, Japan

[5]Faculty of Medicine, Department of Pediatrics, Yamagata University Yamagata, Japan

Received 25 January 2011; Accepted 31 July 2011

We report on a female patient with early infantile epileptic encephalopathy and severe psychomotor disability possessing a de novo balanced translocation t(1;9)(q32;q13). The patient showed clonic convulsions of extremities 2 days after birth. Electroencephalogram (EEG) transiently showed atypical suppression-burst pattern. The seizures evolved to brief tonic spasms, and hypsarrhythmia on EEG was noticed at age of 5 months, indicating the transition to West syndrome. By using fluorescent in situ hybridization (FISH), southern hybridization, and inverse PCR, the translocation breakpoints were successfully determined at the nucleotide level. The 1q32.1 breakpoint was located within a segmental duplication and disrupted the gene encoding Slit-Robo Rho GTPase activating protein 2 (*SRGAP2*). The 9q13 breakpoint was suggested to reside in the heterochromatin region. *Srgap2* has been shown to be specifically expressed in developing brain of rodents, negatively regulate neuronal migration and induce neurite outgrowth and branching. Thus, *SRGAP2* is very likely to play a role in the developing human brain. This is a first report of the *SRGAP2* abnormality associated with early infantile epileptic encephalopathy.

Key words: early infantile epileptic encephalopathy; West syndrome; chromosomal translocation; *SRGAP2*

How to Cite this Article:
Saitsu H, Osaka H, Sugiyama S, Kurosawa K, Mizuguchi T, Nishiyama K, Nishimura A, Tsurusaki Y, Doi H, Miyake N, Harada N, Kato M, Matsumoto N. 2012. Early infantile epileptic encephalopathy associated with the disrupted gene encoding Slit-Robo Rho GTPase activating protein 2 (*SRGAP2*).
Am J Med Genet Part A 158A:199–205.

INTRODUCTION

Many infantile epileptic syndromes show a unique combination of seizure types and electroencephalogram (EEG) findings depending on the patients' age [Kato et al., 2008]. Ohtahara syndrome (OS) and early myoclonic encephalopathy (EME) are characterized by early onset seizures mainly in neonatal period, and suppression-burst pattern on EEG, though their initial seizure type is different [Djukic et al., 2006; Ohtahara and Yamatogi, 2006]. Both OS and EME can progress to the West syndrome phenotype age-dependently, which is characterized by brief tonic spasms, a specific EEG pattern called hypsarrhythmia [Kato, 2006], in 75% and 41% of cases, respectively [Djukic et al., 2006; Ohtahara and Yamatogi, 2006]. The three epileptic syndromes (OS, EME, and West syndrome) are generally intractable and show the arrest of psychomotor development [Djukic et al., 2006; Kato, 2006; Ohtahara and Yamatogi, 2006]. Brain malformations and metabolic disorders were found as underlying causes of the three syndromes, but

Grant sponsor: Ministry of Health, Labour and Welfare; Grant sponsor: Japan Society for the Promotion of Science; Grant sponsor: Yokohama Foundation for Advancement of Medical Science; Grant sponsor: Japan Epilepsy Research Foundation; Grant sponsor: Naito Foundation.

*Correspondence to:
Dr. Hirotomo Saitsu, Department of Human Genetics, Yokohama City University Graduate School of Medicine, Fukuura 3-9, Kanazawa-ku, Yokohama 236-0004, Japan. E-mail: hsaitsu@yokohama-cu.ac.jp

Published online 21 November 2011 in Wiley Online Library (wileyonlinelibrary.com).
DOI 10.1002/ajmg.a.34363

many idiopathic or cryptogenic cases remain etiologically unexplained. Recently, several causative genes have been reported: *ARX* in OS and West syndrome, *CDKL5* in West syndrome, *STXBP1* in OS, *SLC25A22* in EME [Stromme et al., 2002; Kalscheuer et al., 2003; Weaving et al., 2004; Molinari et al., 2005; Kato et al., 2007; Saitsu et al., 2008]. Of note, mutations in *ARX* have been found in both OS and West syndrome phenotypes, suggesting a common pathological seizure mechanism between them. However, there are still large numbers of cases remaining to be elucidated. Identification of new causative genes is absolutely necessary for further understanding of infantile epileptic syndromes.

The Slit-Robo signaling controls the neuronal migration and axonal guidance [Brose et al., 1999; Li et al., 1999; Wu et al., 1999], both of which are dependent on cytoskeletal reorganization. The family of Rho-GTPases, including Rac, Cdc42, and Rho, plays important roles in regulating cytoskeletal dynamics [Hall, 1998]. Rho-GTPases alternate between active (GTP-bound) and inactive (GDP-bound) conformation. The activities of Rho GTPases are tightly and antagonistically regulated by Guanine nucleotide exchange factors (GEFs) and GTPase activating proteins (GAPs): GEFs catalyze nucleotide exchange and mediate activation, while GAPs increase the intrinsic GTPase activities to promote GTP hydrolysis, leading to inactivation [Lamarche and Hall, 1994]. Slit-Robo Rho GTPase activating proteins (SRGAPs) were identified as a family of GAP proteins which bind to the intracellular domain of Robo [Wong et al., 2001]. Three family members (SRGAP1-3) specifically expressed in developing brain of rodents [Wong et al., 2001; Yao et al., 2008; Bacon et al., 2009]. Recent studies suggested that SRGAPs are involved in neuronal development. SRGAP1 protein is required for Slit-mediated repulsion of migratory cells from the anterior subventricular zone of the forebrain by blocking Cdc42 activity [Wong et al., 2001]. Functional disruption of SRGAP3 protein is associated with severe mental retardation in 3p-syndrome [Endris et al., 2002]. Moreover, it has been reported that SRGAP2 negatively regulates neuronal migration and induces neurite outgrowth and branching [Guerrier et al., 2009].

Here, we present a patient with infantile epileptic encephalopathy and profound psychomotor delay with a de novo reciprocal translocation t(1;9)(q32;q13), disrupting the *SRGAP2* gene. Detailed genomic analysis is presented.

CLINICAL REPORT

The 5-year-old girl is a product of unrelated healthy parents. She was born at term without asphyxia after an uneventful pregnancy. She showed apnea twice at day 1. Clonic convulsions of extremities started at day 2. Initial EEG performed at 10-day was reported as normal. Subsequently, myoclonus, which was easily induced by stimulation, was observed. Ictal EEG during myoclonus did not indicate that it was an electronical convulsion. Clonic convulsions were increased at 2 months of age when atypical suppression-burst pattern was transiently observed (Fig. 1A). Her seizures were controlled by combination of vitamin B6, zonisamide, phenobarbital, and KBr, but myoclonus continued. Brain magnetic resonance imaging (MRI) showed cortical atrophy and thin corpus callosum at 2 months of age (Fig. 1C–E). West syndrome was diagnosed at 5 months of age by intellectual disability without head control, series of tonic-spasms, and hypsarrhysmia on EEG (Fig. 1B).

MATERIALS AND METHODS

Molecular Cytogenetic Analysis

G-banded chromosomes of peripheral lymphocytes were analyzed. Fluorescence in situ hybridization (FISH) was performed using peripheral lymphocytes. Labeling, hybridization, wash, and image acquisition were performed as previously described [Saitsu et al., 2008]. RPCI-11 BAC clones and approximately 10-kb probes amplified by long PCR using LA Taq polymerase (Takara Bio, Otsu, Japan) were used as probes. Primer information is available on request.

GeneChip Human Mapping 250K *NspI* Array

Genomic DNA obtained from peripheral blood leukocytes were used for microarray analysis. Experimental procedures were performed according to the manufacturer's protocol with slight modification (fragmentation time was shortened to 25 min). Call rate was 89.5%. Copy number alterations were analyzed by using CNAG2.0 [Nannya et al., 2005].

Cloning of Translocation Breakpoints

The 1q32.1 translocation breakpoint was analyzed by Southern hybridization using *Eco*RI- and *Pst*I-digested patient DNA. Her parental DNAs were also analyzed. Probes were synthesized by PCR DIG probe synthesis kit (Roche, Basel, Switzerland) using RP11-134f21 DNA as a template. Primer information is available on request. Hybridization, washing and detection of probes were done according to the manufacturer's protocol. Images were captured on FluorChem (Alpha Innotech, San Leandro, CA). After identification of aberrant DNA fragments by Southern hybridization, size fractioning of electrophoresed *Eco*RI- and *Pst*I-digested DNA of the patient was performed using QIAEXII Gel extraction kit (Qiagen, Valencia, CA) in order to obtain der(1) and der(9) translocation junction fragments, respectively. The collected DNA was self-ligated by Ligation high (Toyobo, Osaka, Japan), ethanol precipitated and dissolved in 20 μl EB buffer (Qiagen). Inverse PCR was performed in 25 μl of volume, containing 2 μl ligated DNA, 1× LA PCR bufferII, 2.5 mM $MgCl_2$, 0.4 mM each dNTP, 0.5 μM each primer, and 1.25 U LA Taq polymerase (Takara Bio). Primers were listed below: *Eco*RI-forward, 5′-GAAATGGCCTGGCTTGGTTGCTAT-3′; *Eco*RI-reverse, 5′-CACTGAAGCTGCCCTTGAGAAGTGA-3′; *Pst*I-forward, 5′-TTTCCCTCCATGATTCCTCTCTGCT-3′; *Pst*I-reverse, 5′-CCAGGACAGCGTCTCACTCTCCATA-3′. Negative controls only used either forward or reverse primer. The PCR product was purified with ExoSAP (USB Co., Cleveland, OH) and sequenced for both forward and reverse strands with BigDye Terminator chemistry ver. 3 according to the standard protocol (Applied Biosystems, Foster city, CA). After breakpoint sequences were determined, breakpoint-specific primers for both der(1) and der(9) translocation junctions were designed: der(1)-forward, 5′-CCAAGGAATTGGGATCTCTGGGTCT -3′; der(1)-reverse, 5′-CATTCCATTCCATTCCCCTGCAC -3′ (1,098-bp);

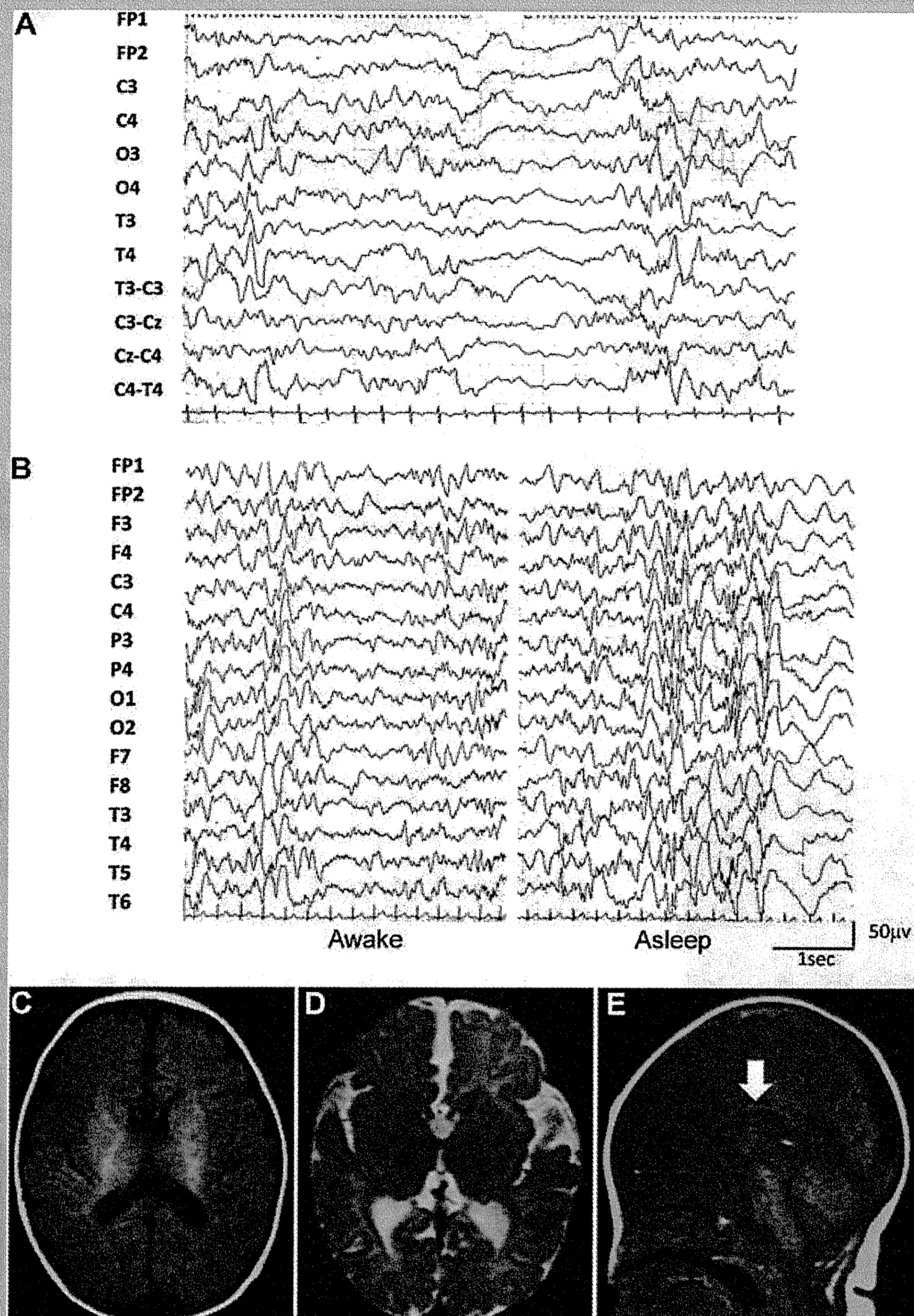

FIG. 1. EEG and brain MRI of the patient. A: Interictal high-voltage bursts alternate with low amplitude suppression phases at an approximately regular rate in both awake and asleep states at age of 2 months. Suppression phases do not exhibit "almost flat pattern" as typical suppression-burst pattern. B: Interictal EEG at 5 months shows multifocal spikes at awake (left), and high-voltage slow rhythm superimposed with irregular spikes; hypsarrhythmia at sleep with some periodicity (right). C,D: Brain MRI T1- (C) and T2-weighted (D) axial images show mild cortical atrophy with normal myelination. E: Sagital brain T1-weighted image shows thin corpus callosum (arrow)

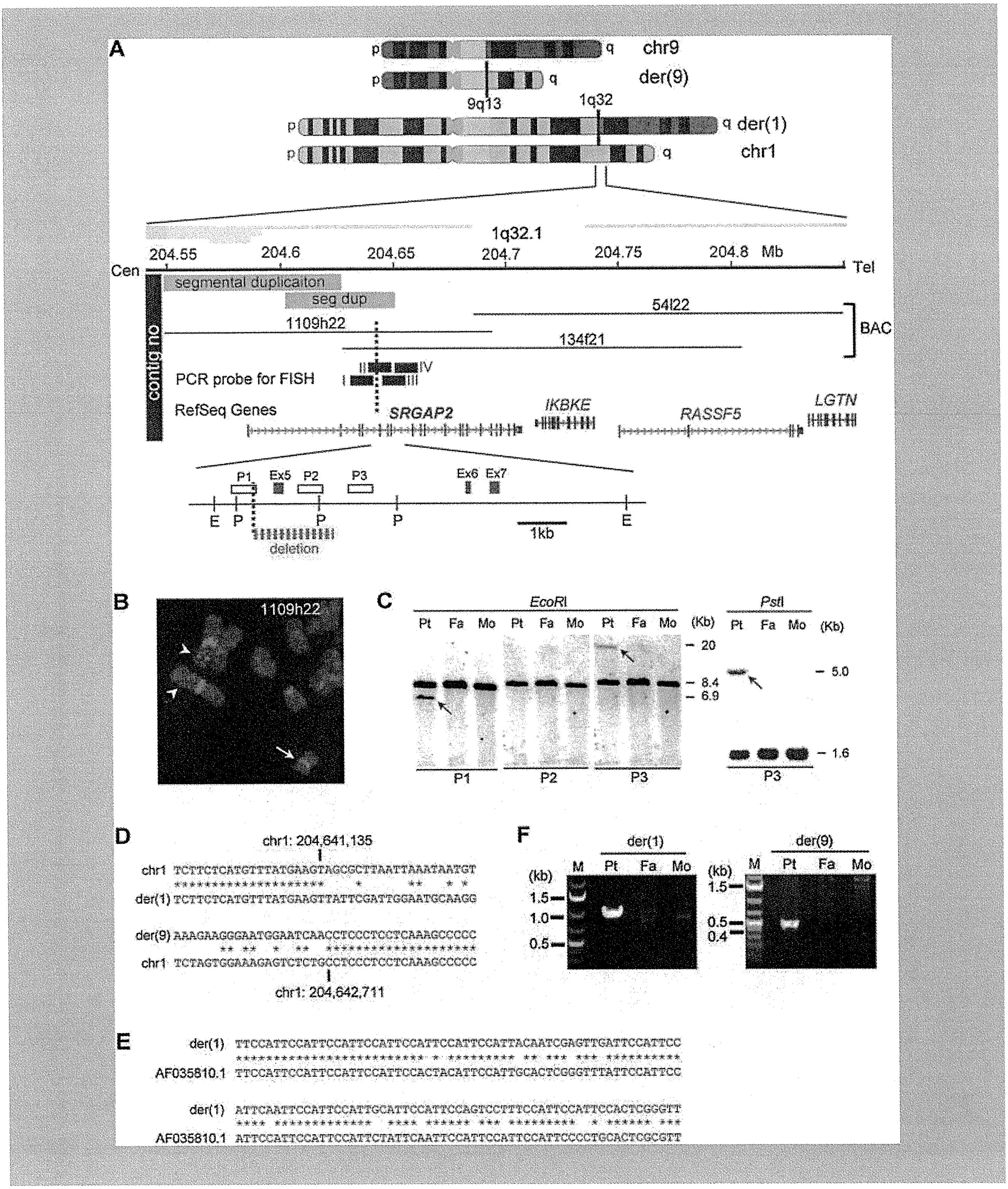
A
chr9
der(9)
9q13
1q32
der(1)
chr1
1q32.1
204.55
204.6
204.65
204.7
204.75
204.8 Mb
Cen
Tel
segmental duplicaiton
seg dup
54I22
1109h22
134f21
BAC
contig no
PCR probe for FISH
RefSeq Genes
SRGAP2
IKBKE
RASSF5
LGTN
P1
Ex5
P2
P3
Ex6
Ex7
1kb
deletion
B
1109h22
C
EcoRI
PstI
Pt Fa Mo
(Kb)
20
8.4
6.9
5.0
1.6
D
chr1: 204,641,135
chr1: 204,642,711
F
der(1)
der(9)
M Pt Fa Mo
(kb)
1.5
1.0
0.5
0.4
E
AF035810.1

der(9)-forward, 5′-GGAAAGGAATGGAATGAAATCAACGCG-3′; der(9)-reverse, 5′-CCAGGACAGCGTCTCACTCTCCATA-3′ (495-bp). Junction fragments were amplified by PCR using these primer-sets on DNAs of the patient and her parents.

RESULTS

G-banded chromosomal analysis revealed a balanced translocation t(1;9)(q32;q13). Her parents showed a normal karyotype (data not shown), indicating that the translocation occurred de novo. Subsequent FISH analysis demonstrated that the breakpoint in chromosome 1 was covered by the clones, RP11-1109h22 and 134f21, showing signals all on normal chromosome 1 and derivatives chromosomes 1 and 9 (Fig. 2A,B). The overlapping region of these two clones was localized within the *SRGAP2* locus (Fig. 2A). The 5′-part of *SRGAP2* transcript was not mapped in the Human Genome browser (both in NCBI Build 36.1/hg18 and GRCh37/hg19 assembly) because the genomic contigs covering the immediately upstream regions of *SRGAP2* gene were absent. Thus, we described the putative exon number based on the order of mappable exons to the existing genomic database. The breakpoint was further narrowed down by FISH analysis using long PCR products as probes (Fig. 2A). Probe II showed weak but clear signals all in on chromosome 1, and derivative chromosomes 1 and 9, suggesting that the breakpoint was located within probe II (data not shown). It was of note that the probe II is associated with a segmental duplication (Fig. 2A). Southern hybridization analysis using probes P1 and P3 detected different aberrant bands only in the patient (Fig. 2A,C), indicating that the 1q32 breakpoint was located at the region between the two probes. P2 did not show any aberrant bands in Southern analysis, suggesting that a small deletion may have occurred near the breakpoint (Fig. 2A,C). Inverse PCR [Triglia et al., 1988] on *Eco*RI- and *Pst*I-digested DNA was successful in obtaining der(1) and der(9) breakpoint-junction fragments, respectively. Sequence analysis showed that the 1q32 translocation breakpoint was located within the putative intron 5 of *SRGAP2*, and exon 5 was completely deleted (Fig. 2A). Sequences of the 9q13 breakpoint were not uniquely mapped to reference sequences. However, sequences of 3′-end of the der(1) junction fragment (approximately 6.1-kb apart from the breakpoint) were similar to satellite 3 sequences (GeneBank accession number AF035810.1) (Fig. 2E), suggesting that 9q13 breakpoint was located in the heterochromatin region. Breakpoint-specific PCR analysis of the patient and her parents confirmed that the rearrangements occurred de novo (Fig. 2F). To check genomic copy number alterations accompanied by the rearrangement, GeneChip Human Mapping 250K *Nsp*I (Affymetrix, Santa Clara, CA) was performed. Besides two known copy number variations, no other imbalances were detected (data not shown).

DISCUSSION

SRGAP2 is a member of Slit-Robo Rho GTPase activating proteins with three domains: an N-terminal F-BAR domain, a RhoGAP domain, and an SH3 domain [Wong et al., 2001; Guerrier et al., 2009]. There are three variants of *SRGAP2* transcripts in humans: variant 1 (GenBank accession number NM_015326.2), variant 2 (GenBank accession number NM_001042758.1), and variant 3 (GenBank accession number NM_001170637.1). In all three variants, the coding proteins commonly possess F-BAR, RhoGAP, and SH3 domains except for an amino acid deletion in F-BAR domain in variant 2. Mouse *Srgap2* is expressed in the entire developing cortex including proliferative zones and postmitotic regions [Bacon et al., 2009; Guerrier et al., 2009]. It has been reported that the SRGAP2 protein negatively regulates neuronal migration and induce neurite outgrowth and branching through its F-BAR domain [Guerrier et al., 2009]. In addition, GAP activity of the SRGAP2 protein specifically downregulate Rac1 [Guerrier et al., 2009]. Mutations in *ARHGEF6*, Rac1/Cdc42 specific GEF, cause X-linked mental retardation [Kutsche et al., 2000]. Moreover, mutation and/or disruption of *OPHN1* and *SRGAP3*, both encoding Rac1-GAPs, are associated with severe mental retardation [Billuart et al., 1998; Endris et al., 2002], indicating the importance of Rac1 regulation in human brain development. Thus, SRGAP2 is likely to play important roles in developing brain in humans through the ability of the F-BAR and RhoGAP domains. It would be interesting to analyze

FIG. 2. Genomic characterization of t(1;9)(q32;q13). A: Schematic representation of the reciprocal translocation, t(1;9)(q32;q13) (top). A summarized physical map covering the 1q32.1 translocation breakpoint is indicated (middle). RP11-1109h22 and 134f21, and PCR probe II span the translocation breakpoint (longitudinal dashed line) in association with the segmental duplication. Four RefSeq genes, including *SRGAP2* spanning the breakpoint, are presented. Note that absence of genomic contigs of the immediately upstream region of the *SRGAP2* gene. More detailed maps are shown (bottom). A partial restriction map (E, *Eco*RI; P, *Pst*I), probes for southern hybridization (P1–P3), and putative exons 5–7 of *SRGAP2* are indicated. Translocation breakpoint (longitudinal dashed line) accompanied with a 1,575-bp deletion encompassing exon 5 of *SRGAP2* (red thick dashed line) are located between P1 and P3. B: FISH analysis using RP11-1109h22 as a probe showed clear signals on chromosome 1, and der(1) (white arrowheads) and der(9) chromosomes (white arrow). Cross-hybridization was also observed to segmental duplications located at pericentric regions of chromosome 1 and derivative chromosome 1. C: Southern hybridization using probes P1, P2, and P3 on genomic DNAs of the patient and her parents. Arrow shows aberrant bands specific to the patient (not observed in parental DNA). Pt, patient; Fa, father; Mo, mother. D: Breakpoint junction sequences of der(1) and der(9). In upper part, top and bottom sequence strands show chromosome 1 and derivative chromosome 1 sequences, respectively. In lower part, top and bottom strands show derivative chromosome 9 and normal chromosome 1 sequences, respectively. Breakpoint positions are marked with small longitudinal lines based on the UCSC genome browser coordinate (version Mar. 2006). Asterisks indicate nucleotides identical to normal chromosomes. E: Sequences of the 3′-end of the der(1) junction fragment. Top and bottom sequence strands show der(1) and satellite 3 sequences, respectively, showing homology between two sequences. F: Breakpoint-specific PCR analysis of the patient's family. Primers specific to der(1) and der(9) breakpoints could successfully amplify 1,098- and 495-bp products, respectively, only from the patient (Pt), indicating the translocation occurred de novo. M, size marker; Fa, father; Mo, mother.

SRGAP2 in a large cohort of patients presenting with early epileptic encephalopathy including West syndrome. Although full-length *SRGAP2* transcripts (functional), which include sequences of putative exons 1–20 at 1q32.1, have been deposited in GeneBank, 5′-part of the *SRGAP2* transcript is not mapped in the Human Genome browser. Furthermore, seven exons of *SRGAP2* were again mapped to two separated segmental duplications at 1q21.1 and 1p11.2 with sequence similarities of 99.29% and 99.30%, respectively (Fig. 2A). This complex genomic structure interfered with full-blown mutation screening especially for the 1,356-bp coding region including the F-BAR domain. A microdeletion within two separate segmental duplications in *SRGAP2* locus has been found in 2 out of 90 Yoruban individuals (presumably with normal phenotype) from the HapMap Project using custom high-density oligonucleotide arrays [Matsuzaki et al., 2009]. However, it is uncertain whether they could confirm the precise locations of the deletions by another method. Thus, there remains a possibility that the deletion actually ocurred at highly homologous genomic segments located at 1q21.1 and 1p11.2. Further descriptions about aberrations of the *SRGAP2* gene will be required for establishing in a causative role in early infantile epileptic encephalopathy.

The 9q13 breakpoint is likely to reside within the heterochromatic region. It is possible that some genes adjacent to 1q32.1 breakpoint would suffer from gene silencing by the position effect. *IKBKE* is an IKK (inhibitor of nuclear factor kappaB kinase)-related kinase that is essential for interferon-inducible antiviral transcriptional response [Tenoever et al., 2007]. *Ikbke* knockout mice are protected from high-fat diet-induced obesity, chronic inflammation in liver and fat, hepatic steatosis, and whole-body insulin resistance [Chiang et al., 2009]. However, neurological abnormalities have never been reported. *RASSF5* is a member of the Ras association domain family. A crutial role in the integrin-mediated adhesion and migration of lymphocytes and dendritic cells has been shown in *Rassf5*-deficient mice, but neurological abnormalities have never been mentioned [Katagiri et al., 2004]. Thus, *IKBKE* and *RASSF5*, two adjacent genes to *SRGAP2*, are less likely to be involved in infantile epileptic encephalopathy.

In conclusion, we described a patient with early infantile epilepsitic encephalopathy, carrying a de novo reciprocal translocation disrupting the *SRGAP2* gene. Clonic convulsions and atypical suppression-burst patterns on EEG at early infantile period did not fit into either OS or EME. However, the seizures became brief tonic spasms, and hypsarrhythmia on EEG was noticed, indicating transition to West syndrome. Disruption of *SRGAP2* may be related to West syndrome which has heterogeneous backgrounds [Kato, 2006].

ACKNOWLEDGMENTS

We would like to thank the patient and her families for their participation in this study. This work was supported by Research Grants from the Ministry of Health, Labour and Welfare (H.S. and N. Matsumoto), Grant-in-Aid for Scientific Research from Japan Society for the Promotion of Science (N. Matsumoto), Grant-in-Aid for Young Scientist from Japan Society for the Promotion of Science (H.S.), Research Promotion Fund from Yokohama Foundation for Advancement of Medical Science (H.S.), Research Grants from the Japan Epilepsy Research Foundation (H.S.), and Research Grant from Naito Foundation (N. Matsumoto).

REFERENCES

Bacon C, Endris V, Rappold G. 2009. Dynamic expression of the Slit-Robo GTPase activating protein genes during development of the murine nervous system. J Comp Neurol 513:224–236.

Billuart P, Bienvenu T, Ronce N, des Portes V, Vinet MC, Zemni R, Roest Crollius H, Carrie A, Fauchereau F, Cherry M, Briault S, Hamel B, Fryns JP, Beldjord C, Kahn A, Moraine C, Chelly J. 1998. Oligophrenin-1 encodes a rhoGAP protein involved in X-linked mental retardation. Nature 392:923–926.

Brose K, Bland KS, Wang KH, Arnott D, Henzel W, Goodman CS, Tessier-Lavigne M, Kidd T. 1999. Slit proteins bind Robo receptors and have an evolutionarily conserved role in repulsive axon guidance. Cell 96:795–806.

Chiang SH, Bazuine M, Lumeng CN, Geletka LM, Mowers J, White NM, Ma JT, Zhou J, Qi N, Westcott D, Delproposto JB, Blackwell TS, Yull FE, Saltiel AR. 2009. The protein kinase IKKepsilon regulates energy balance in obese mice. Cell 138:961–975.

Djukic A, Lado FA, Shinnar S, Moshe SL. 2006. Are early myoclonic encephalopathy (EME) and the Ohtahara syndrome (EIEE) independent of each other? Epilepsy Res 70:S68–S76.

Endris V, Wogatzky B, Leimer U, Bartsch D, Zatyka M, Latif F, Maher ER, Tariverdian G, Kirsch S, Karch D, Rappold GA. 2002. The novel Rho-GTPase activating gene MEGAP/ srGAP3 has a putative role in severe mental retardation. Proc Natl Acad Sci USA 99:11754–11759.

Guerrier S, Coutinho-Budd J, Sassa T, Gresset A, Jordan NV, Chen K, Jin WL, Frost A, Polleux F. 2009. The F-BAR domain of srGAP2 induces membrane protrusions required for neuronal migration and morphogenesis. Cell 138:990–1004.

Hall A. 1998. Rho GTPases and the actin cytoskeleton. Science 279: 509–514.

Kalscheuer VM, Tao J, Donnelly A, Hollway G, Schwinger E, Kubart S, Menzel C, Hoeltzenbein M, Tommerup N, Eyre H, Harbord M, Haan E, Sutherland GR, Ropers HH, Gecz J. 2003. Disruption of the serine/ threonine kinase 9 gene causes severe X-linked infantile spasms and mental retardation. Am J Hum Genet 72:1401–1411.

Katagiri K, Ohnishi N, Kabashima K, Iyoda T, Takeda N, Shinkai Y, Inaba K, Kinashi T. 2004. Crucial functions of the Rap1 effector molecule RAPL in lymphocyte and dendritic cell trafficking. Nat Immunol 5:1045–1051.

Kato M. 2006. A new paradigm for West syndrome based on molecular and cell biology. Epilepsy Res 70:S87–S95.

Kato M, Saitoh S, Kamei A, Shiraishi H, Ueda Y, Akasaka M, Tohyama J, Akasaka N, Hayasaka K. 2007. A longer polyalanine expansion mutation in the ARX gene causes early infantile epileptic encephalopathy with suppression-burst pattern (Ohtahara syndrome). Am J Hum Genet 81: 361–366.

Kato M, Saitoh S, Kamei A, Shiraishi H, Ueda Y, Akasaka M, Tohyama J, Akasaka N, Hayasaka K., 2008. Genetic etiology of age-dependent epileptic encephalopathy in infancy: Longer polyalanine expansion in ARX causes earlier onset and more severe phenotype. In: Takahashi T, Fukuyama Y, editors. Biology of seizure susceptibility in developing brain. Montrouge, Paris: John Libbey Eurotext. pp. 75–86.

Kutsche K Yntema H Brandt A Jantke I Nothwang HG Orth U Boavida MG David D Chelly J Fryns JP Moraine C Ropers HH Hamel BC van Bokhoven H Gal A 2000 Mutations in ARHGEF6 encoding a guanine nucleotide exchange factor for Rho GTPases in patients with X-linked mental retardation Nat Genet 26:247–250.

Lamarche N, Hall A. 1994. GAPs for rho-related GTPases. Trends Genet 10:436–440.

Li HS, Chen JH, Wu W, Fagaly T, Zhou L, Yuan W, Dupuis S, Jiang ZH, Nash W, Gick C, Ornitz DM, Wu JY, Rao Y. 1999. Vertebrate slit, a secreted ligand for the transmembrane protein roundabout, is a repellent for olfactory bulb axons. Cell 96:807–818.

Matsuzaki H, Wang PH, Hu J, Rava R, Fu GK. 2009. High resolution discovery and confirmation of copy number variants in 90 Yoruba Nigerians. Genome Biol 10:R125.

Molinari F, Raas-Rothschild A, Rio M, Fiermonte G, Encha-Razavi F, Palmieri L, Palmieri F, Ben-Neriah Z, Kadhom N, Vekemans M, Attie-Bitach T, Munnich A, Rustin P, Colleaux L. 2005. Impaired mitochondrial glutamate transport in autosomal recessive neonatal myoclonic epilepsy. Am J Hum Genet 76:334–339.

Nannya Y, Sanada M, Nakazaki K, Hosoya N, Wang L, Hangaishi A, Kurokawa M, Chiba S, Bailey DK, Kennedy GC, Ogawa S. 2005. A robust algorithm for copy number detection using high-density oligonucleotide single nucleotide polymorphism genotyping arrays. Cancer Res 65: 6071–6079.

Ohtahara S, Yamatogi Y. 2006. Ohtahara syndrome: With special reference to its developmental aspects for differentiating from early myoclonic encephalopathy. Epilepsy Res 70:S58–S67.

Saitsu H, Kato M, Mizuguchi T, Hamada K, Osaka H, Tohyama J, Uruno K, Kumada S, Nishiyama K, Nishimura A, Okada I, Yoshimura Y, Hirai S, Kumada T, Hayasaka K, Fukuda A, Ogata K, Matsumoto N. 2008. De novo mutations in the gene encoding STXBP1 (MUNC18-1) cause early infantile epileptic encephalopathy. Nat Genet 40:782–788.

Stromme P, Mangelsdorf ME, Shaw MA, Lower KM, Lewis SM, Bruyere H, Lutcherath V, Gedeon AK, Wallace RH, Scheffer IE, Turner G, Partington M, Frints SG, Fryns JP, Sutherland GR, Mulley JC, Gecz J. 2002. Mutations in the human ortholog of Aristaless cause X-linked mental retardation and epilepsy. Nat Genet 30:441–445.

Tenoever BR, Ng SL, Chua MA, McWhirter SM, Garcia-Sastre A, Maniatis T. 2007. Multiple functions of the IKK-related kinase IKKepsilon in interferon-mediated antiviral immunity. Science 315:1274–1278.

Triglia T, Peterson MG, Kemp DJ. 1988. A procedure for in vitro amplification of DNA segments that lie outside the boundaries of known sequences. Nucleic Acids Res 16:8186.

Weaving LS, Christodoulou J, Williamson SL, Friend KL, McKenzie OL, Archer H, Evans J, Clarke A, Pelka GJ, Tam PP, Watson C, Lahooti H, Ellaway CJ, Bennetts B, Leonard H, Gecz J. 2004. Mutations of CDKL5 cause a severe neurodevelopmental disorder with infantile spasms and mental retardation. Am J Hum Genet 75:1079–1093.

Wong K, Ren XR, Huang YZ, Xie Y, Liu G, Saito H, Tang H, Wen L, Brady-Kalnay SM, Mei L, Wu JY, Xiong WC, Rao Y. 2001. Signal transduction in neuronal migration: Roles of GTPase activating proteins and the small GTPase Cdc42 in the Slit-Robo pathway. Cell 107:209–221.

Wu W, Wong K, Chen J, Jiang Z, Dupuis S, Wu JY, Rao Y. 1999. Directional guidance of neuronal migration in the olfactory system by the protein Slit. Nature 400:331–336.

Yao Q, Jin W-L, Wang Y, Ju G. 2008. Regulated shuttling of Slit-Robo-GTPase activating proteins between nucleus and cytoplasm during brain development. Cell Mol Neurobiol 28:205–221.

RESEARCH ARTICLE

AMERICAN JOURNAL OF
medical genetics

Spectrum of *MLL2* (*ALR*) Mutations in 110 Cases of Kabuki Syndrome

Mark C. Hannibal,[1,2] Kati J. Buckingham,[1] Sarah B. Ng,[3] Jeffrey E. Ming,[4] Anita E. Beck,[1,2] Margaret J. McMillin,[2] Heidi I. Gildersleeve,[1] Abigail W. Bigham,[1] Holly K. Tabor,[1,2] Heather C. Mefford,[1,2] Joseph Cook,[1] Koh-ichiro Yoshiura,[5] Tadashi Matsumoto,[5] Naomichi Matsumoto,[6] Noriko Miyake,[6] Hidefumi Tonoki,[7] Kenji Naritomi,[8] Tadashi Kaname,[8] Toshiro Nagai,[9] Hirofumi Ohashi,[10] Kenji Kurosawa,[11] Jia-Woei Hou,[12] Tohru Ohta,[13] Deshung Liang,[14] Akira Sudo,[15] Colleen A. Morris,[16] Siddharth Banka,[17] Graeme C. Black,[17] Jill Clayton-Smith,[17] Deborah A. Nickerson,[3] Elaine H. Zackai,[4] Tamim H. Shaikh,[18] Dian Donnai,[17] Norio Niikawa,[13] Jay Shendure,[3] and Michael J. Bamshad[1,2,3]*

[1]Department of Pediatrics, University of Washington, Seattle, Washington

[2]Seattle Children's Hospital, Seattle, Washington

[3]Department of Genome Sciences, University of Washington, Seattle, Washington

[4]Department of Pediatrics, The Children's Hospital of Philadelphia, The University of Pennsylvania School of Medicine, Philadelphia, Pennsylvania

[5]Department of Human Genetics, Nagasaki University Graduate School of Biomedical Sciences, Nagasaki, Japan

[6]Department of Human Genetics, Yokohama City University Graduate School of Medicine, Yokohama, Japan

[7]Department of Pediatrics, Tenshi Hospital, Sapporo, Japan

[8]Department of Medical Genetics, University of the Ryukyus, Okinawa, Japan

[9]Department of Pediatrics, Dokkyo Medical University, Koshigaya Hospital, Saitama, Japan

[10]Division of Medical Genetics, Saitama Children's Medical Center, Saitama, Japan

[11]Division of Clinical Genetics, Kanagawa Children's Medical Center, Yokohama, Japan

[12]Department of Pediatrics, Chang Gung Children's Hospital, Taoyuan, Taiwan, Republic of China

[13]Research Institute of Personalized Health Sciences, Health Sciences University of Hokkaido, Hokkaido, Japan

[14]National Laboratory of Medical Genetics, Xiangya Hospital, Central South University, Republic of China

[15]Department of Pediatrics, Sapporo City General Hospital, Sapporo, Japan

[16]University of Nevada School of Medicine, Las Vegas, Nevada

[17]Department of Genetic Medicine, Manchester Academic Health Sciences Centre, University of Manchester, England

[18]Department of Pediatrics, University of Colorado, Denver, Colorado

Received 25 February 2011; Accepted 30 March 2011

Additional supporting information may be found in the online version of this article.

Grant sponsor: National Institutes of Health/National Heart Lung and Blood Institute; Grant number: 5R01HL094976; Grant sponsor: National Institutes of Health/National Human Genome Research Institute; Grant numbers: 5R21HG004749, 1RC2HG005608, 5RO1HG004316, T32HG00035; Grant sponsor: National Institute of Heath/National Institute of Environmental Health Sciences; Grant number: HHSN273200800010C; Grant sponsor: National Institute of Neurological Disorders and Stroke; Grant number: RO1NS35102; Grant sponsor: NIHR Manchester Biomedical Research Centre; Grant sponsor: Ministry of Health, Labour and Welfare of Japan; Grant sponsor: Japan Science and Technology Agency; Grant sponsor: Society for the Promotion of Science; Grant sponsor: Life Sciences Discovery Fund; Grant numbers: 2065508, 0905001; Grant sponsor: Washington Research Foundation; Grant sponsor: National Institutes of Health/ National Institute of Child Health and Human Development; Grant numbers: 1R01HD048895, 5K23HD057331.

Mark C. Hannibal, Kati J. Buckingham, and Sarah B. Ng contributed equally to this work.

*Correspondence to:
Michael J. Bamshad, M.D., Department of Pediatrics, University of Washington School of Medicine, Box 356320, 1959 NE Pacific Street, Seattle, WA 98195. E-mail: mbamshad@u.washington.edu

Published online 10 June 2011 in Wiley Online Library (wileyonlinelibrary.com).
DOI 10.1002/ajmg.a.34074

Kabuki syndrome is a rare, multiple malformation disorder characterized by a distinctive facial appearance, cardiac anomalies, skeletal abnormalities, and mild to moderate intellectual disability. Simplex cases make up the vast majority of the reported cases with Kabuki syndrome, but parent-to-child transmission in more than a half-dozen instances indicates that it is an autosomal dominant disorder. We recently reported that Kabuki syndrome is caused by mutations in *MLL2*, a gene that encodes a Trithorax-group histone methyltransferase, a protein important in the epigenetic control of active chromatin states. Here, we report on the screening of 110 families with Kabuki syndrome. *MLL2* mutations were found in 81/110 (74%) of families. In simplex cases for which DNA was available from both parents, 25 mutations were confirmed to be de novo, while a transmitted *MLL2* mutation was found in two of three familial cases. The majority of variants found to cause Kabuki syndrome were novel nonsense or frameshift mutations that are predicted to result in haploinsufficiency. The clinical characteristics of *MLL2* mutation-positive cases did not differ significantly from *MLL2* mutation-negative cases with the exception that renal anomalies were more common in *MLL2* mutation-positive cases. These results are important for understanding the phenotypic consequences of *MLL2* mutations for individuals and their families as well as for providing a basis for the identification of additional genes for Kabuki syndrome.

Key words: Kabuki syndrome; *MLL2*; *ALR*; Trithorax group histone methyltransferase

How to Cite this Article:
Hannibal MC, Buckingham KJ, Ng SB, Ming JE, Beck AE, McMillin MJ, Gildersleeve HI, Bigham AW, Tabor HK, Mefford HC, Cook J, Yoshiura K-i, Matsumoto T, Matsumoto N, Miyake N, Tonoki H, Naritomi K, Kaname T, Nagai T, Ohashi H, Kurosawa K, Hou J-W, Ohta T, Liang D, Sudo A, Morris CA, Banka S, Black GC, Clayton-Smith J, Nickerson DA, Zackai EH, Shaikh TH, Donnai D, Niikawa N, Shendure J, Bamshad MJ. 2011. Spectrum of *MLL2* (*ALR*) mutations in 110 cases of Kabuki syndrome.

Am J Med Genet Part A 155:1511–1516.

INTRODUCTION

Kabuki syndrome (OMIM#147920) is a rare, multiple malformation disorder characterized by a distinctive facial appearance, cardiac anomalies, skeletal abnormalities, and mild to moderate intellectual disability. It was originally described by Niikawa et al. [1981] and Kuroki et al. [1981] in 1981, and to date, about 400 cases have been reported worldwide [Niikawa et al., 1988; White et al., 2004; Adam and Hudgins, 2005]. The spectrum of abnormalities found in individuals with Kabuki syndrome is diverse, yet virtually all affected persons are reported to have similar facial features consisting of elongated palpebral fissures, eversion of the lateral third of the lower eyelids, and broad, arched eyebrows with lateral sparseness. Additionally, affected individuals commonly have severe feeding problems, failure to thrive in infancy, and height around or below the 3rd centile for age in about half of cases.

We recently reported that a majority of cases of Kabuki syndrome are caused by mutations in *mixed lineage leukemia 2* (*MLL2*; OMIM#602113), also known as either *MLL4* or *ALR* [Ng et al., 2010]. *MLL2* encodes a SET-domain-containing histone methyltransferase important in the epigenetic control of active chromatin states [FitzGerald and Diaz, 1999]. Exome sequencing revealed that 9 of 10 individuals had novel variants in *MLL2* that were predicted to be deleterious. A single individual had no mutation in the protein-coding exons of *MLL2*, though in retrospect, his phenotypic features are somewhat atypical of Kabuki syndrome. In a larger validation cohort screened by Sanger sequencing, we found *MLL2* mutations in approximately two-thirds of 43 Kabuki cases, suggesting that Kabuki syndrome is genetically heterogeneous.

Herein we report on the results of screening *MLL2* for mutations in 110 families with one or more individuals affected with Kabuki syndrome in order to: (1) characterize the spectrum of *MLL2* mutations that cause Kabuki syndrome; (2) determine whether *MLL2* genotype is predictive of phenotype; (3) assess whether the clinical characteristics of *MLL2* mutation-positive cases differ from *MLL2* mutation-negative cases; and (4) delineate the subset of Kabuki cases that are *MLL2* mutation-negative for further gene discovery studies.

MATERIALS AND METHODS

Subjects

Referral for inclusion into the study required a diagnosis of Kabuki syndrome made by a clinical geneticist. From these cases, phenotypic data were collected by review of medical records, phone interviews, and photographs. These data were collected from five different clinical genetics centers in three different countries and over a protracted period of time and forwarded for review to two of the authors (M.B. and M.H.). Data on certain phenotypic characteristics including stature, feeding difficulties, and failure to thrive was not uniformly collected or standardized. Therefore, we decided to be conservative in our analysis and use only phenotypic traits that could be represented by discrete variables (i.e., presence or absence) and for which data were available from at least 70% of cases. In addition, these clinical summaries were de-identified and therefore facial photographs were unavailable from most cases studied. Written consent was obtained for all participants who provided identifiable samples. The Institutional Review Boards of Seattle Children's Hospital and the University of Washington approved all studies. A summary of the clinical characteristics of 53 of these individuals diagnosed with Kabuki syndrome has been reported previously [Ng et al., 2010].

Mutation Analysis

Genomic DNA was extracted using standard protocols. Each of the 54 exons of *MLL2* was amplified using Taq DNA polymerase (Invitrogen, Carlsbad, CA) following manufacturer's recommendations and using primers previously reported [Ng et al., 2010]. PCR products were purified by treatment with exonuclease I (New England Biolabs, Inc., Beverly, MA) and shrimp alkaline phosphatase (USB Corp., Cleveland, OH), and products were sequenced using the dideoxy terminator method on an automated sequencer (ABI 3130xl). The electropherograms of both forward and reverse strands were manually reviewed using CodonCode Aligner (Dedham, MA). Primer sequences and conditions are listed in Supplementary Table I.

For *MLL2* mutation-negative samples, DNA was hybridized to commercially available whole-genome tiling arrays consisting of one million oligonucleotide probes with an average spacing of 2.6 kb throughout the genome (SurePrint G3 Human CGH Microarray 1 × 1 M, Agilent Technologies, Santa Clara, CA). Twenty-one probes on this array covered *MLL2* specifically. Data were analyzed using Genomics Workbench software according to manufacturer's instructions.

RESULTS

All 54 protein-coding exons and intron–exon boundaries of *MLL2* were screened by Sanger sequencing in a cohort of 110 kindreds with Kabuki syndrome. This cohort included 107 simplex cases (including a pair of monozygotic twins) and 3 familial (i.e., parent-offspring) cases putatively diagnosed with Kabuki syndrome. Seventy novel *MLL2* variants that were inferred to be disease-causing were identified in 81/110 (74%) kindreds (Fig. 1 and Supplementary Table II online). These 81 mutations included 37 nonsense mutations (32 different sites and five sites with recurrent mutations), 3 in-frame deletions or duplications (2 different sites and 1 site with a recurrent mutation), 22 frameshifts (22 different sites), 16 missense mutations (11 different sites and 4 sites with recurrent mutations), and 3 splice consensus site (or intron–exon boundary) mutations. None of these variants were found in dbSNP (build 132), the 1000 Genomes Project pilot data, or 190 chromosomes from individuals matched for geographical ancestry. In total, pathogenic variants were found at 70 sites. Additionally, there were 10 sites at which recurrent mutations were observed.

For 25 simplex cases in which we identified *MLL2* mutations, DNA was available from both unaffected parents, and in each case the mutation was confirmed to have arisen de novo (Supplementary Table II online). These included 14 nonsense, 5 frameshift, 3 missense, 2 splice site mutations, and 1 deletion. De novo events were confirmed at 6 of the 10 sites where recurrent mutations were noted. In addition to the 81 kindreds in which we identified causal *MLL2* mutations, we found two *MLL2* variants in each of three simplex cases. In each case, neither *MLL2* mutation could unambiguously

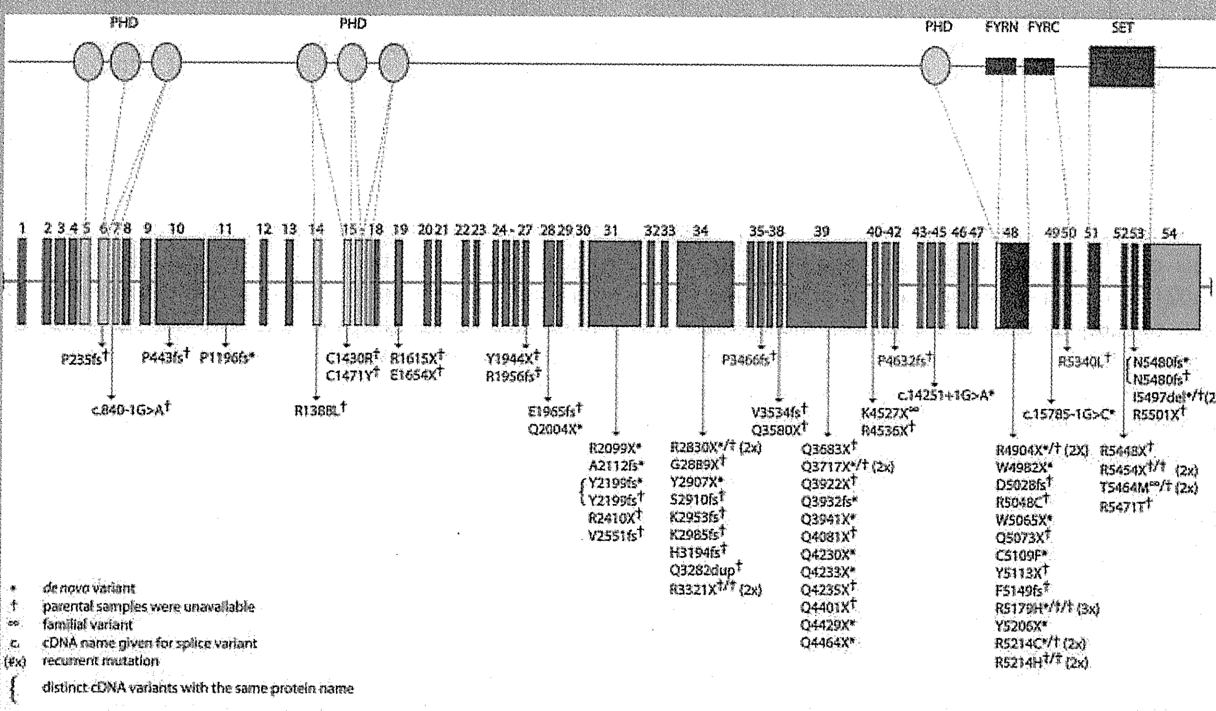

FIG. 1. Genomic structure and allelic spectrum of *MLL2* mutations that cause Kabuki syndrome. *MLL2* is composed of 54 exons that include untranslated regions (orange) and protein coding sequence (blue) including 7 PHD fingers (yellow), FYRN (green), FYRC (green), and a SET domain (red). Arrows indicate the locations of 81 mutations affecting 70 sites found in 110 families with Kabuki syndrome including: 37 nonsense, 22 frameshifts, 16 missense, 3 in-frame deletions/duplications, and 3 splice-site mutations. Asterisks indicate mutations that were confirmed to be de novo and crosses indicate cases for which parental DNA was unavailable. Figure adapted from Ng et al. [2010].

be defined as disease-causing (Supplementary Table II online). In one case, we found both a 21 bp in-frame insertion in exon 39 and a 1 bp insertion in exon 46 predicted to cause a frameshift. However, the unaffected mother also carried the 21 bp insertion suggesting that this is a rare polymorphism, and that the 1 bp deletion is the pathogenic mutation responsible for Kabuki syndrome.

Apparent disease-causing variants were discovered in nearly half (i.e., 22/54) of all protein-coding exons of *MLL2* and in virtually every region known to encode a functional domain (Fig. 1). However, the distribution of variants appeared non-random as 13 and 12 novel variants were identified in exons 48 and 39, respectively. These sites accounted for 25, or more than one-third, of all the novel *MLL2* variants and 31/81 mutations that cause Kabuki syndrome in our cohort. Eleven of the 12 pathogenic variants in exon 39 were nonsense mutations and occurred in regions that encode long polyglutamine tracts.

Four of the families studied herein had two individuals affected with Kabuki syndrome. A pair of monozygous twins with a c.15195G>A nonsense mutation were concordant for mild developmental delay, congenital heart disease, preauricular pits, and palatal abnormalities, but discordant for hearing loss, and a central nervous system malformation. Concordance for mild developmental delay between an affected parent and child was observed in two families with *MLL2* mutations, one with a nonsense mutation, c.13579A>T, p.K4527X, and the other with a missense mutation, c.16391C>T, p.T5464M that was also found in a simplex case. No *MLL2* mutation was found in the remaining affected parent and child pair (Fig. 2).

To examine the relationship between genotype and phenotype, we first compared the frequency of developmental delay, congenital heart disease, cleft lip and/or palate, and structural renal defects between *MLL2* mutation-positive versus *MLL2* mutation-negative cases. No significant difference was observed between groups for three of these four phenotypes (Table Ia). However, renal anomalies were observed in 47% (31/66 cases) of *MLL2* mutation-positive cases compared to 14% (2/14 cases) of *MLL2* mutation-negative cases and this difference was statistically significant ($\chi^2 = 5.1$, df $= 1$, $P = 0.024$). In 35 cases in two clinical cohorts for whom more complete phenotypic data were available, short stature was observed in 54% (14/26) of *MLL2* mutation-positive cases compared to 33% (3/19 cases) of *MLL2* mutation-negative cases. We also divided the *MLL2* mutation-positive cases into those with nonsense and frameshift mutations and those with missense mutations and compared the frequency of developmental delay, congenital heart disease, cleft lip and/or palate, and structural renal defects between groups. No significant differences were observed between groups (Table Ib).

In 26 independent cases of Kabuki syndrome, including one parent -offspring pair, no *MLL2* mutation was identified. Both persons in the mother–child pair had facial characteristics consistent with Kabuki syndrome (Fig. 2), mild developmental delay, and no major malformations. The mother is of Cambodian ancestry and her daughter is of Cambodian and European American ancestry. In general, most of the *MLL2* mutation-negative Kabuki cases had facial characteristics (Fig. 3) similar to those of the *MLL2* mutation-positive Kabuki cases, and a similar pattern of major malformations (Table I) with the exception of fewer renal abnormalities.

TABLE I. Phenotypic Traits Grouped by *MLL2* Mutation Status (a) and Type (b)

Trait	*MLL2* +	*MLL2* −
Intellectual disability	74/74 (100%)	19/20 (95%)
Mild	51/74 (69%)	10/20 (50%)
Moderate	18/74 (24%)	4/20 (20%)
Severe	4/74 (5%)	3/20 (15%)
Cleft palate, CL/CP	29/72 (40%)	8/18 (44%)
Congenital heart defect	36/71 (51%)	8/19 (42%)
Renal abnormality	31/66 (47%)	2/14 (14%)

Trait	Truncating (N = 59)	Missense (N = 16)
Intellectual disability	54/54 (100%)	15/15 (100%)
Mild	36/54 (67%)	11/15 (73%)
Moderate	13/54 (24%)	4/15 (27%)
Severe	5/54 (9%)	0/15
Cleft palate, CL/CP	23/54 (43%)	3/14 (21%)
Congenital heart defect	30/54 (55%)	4/13 (30%)
Renal anomaly	9/44 (20%)	2/12 (17%)

We screened the *MLL2* mutation-negative cases by aCGH for large deletions or duplications that encompassed *MLL2*. Abnormalities were found in four cases. In one case, a 1.87 kb deletion of chromosome 5 (hg18, chr5:175,493,803–177,361,744) that included *NSD1* and had breakpoints in flanking segmental duplications identical to the microdeletion commonly found in Sotos syndrome, was found. This suggests that this individual has Sotos syndrome, not Kabuki syndrome [Kurotaki et al., 2002]. A second case had a novel 977-kb deletion of chromosome 19q13 (hg18, chr19:61,365,420–62,342,064) encompassing 20 genes. The majority of genes within the deleted region are zinc finger genes, some of which are known to be imprinted in both human and mouse. A third case had a complex translocation t(8;18)(q22;q21). Finally, a fourth case was found to have extra material for the entire chromosome 12. Average log 2 ratio across chromosome 12 was 0.49, most likely representing mosaic aneuploidy of chromosome 12. No aCGH abnormalities were observed in 21 cases and aCGH failed for one case.

DISCUSSION

We have expanded the spectrum of mutations in *MLL2* that cause Kabuki syndrome and explored the relationship between *MLL2* genotype and some of the major, objective phenotypic characteristics of Kabuki syndrome. The majority of variants found to cause Kabuki syndrome are either novel nonsense or frameshift mutations, and appear to arise de novo. While mutations that cause Kabuki syndrome are found throughout the *MLL2* gene, there appear to be at least two exons (39 and 48) in which mutations are identified with a considerably higher frequency. Mutations in these two exons account for nearly half of all mutations found in *MLL2*, while the length of these exons represents ~24% of the *MLL2* open reading frame (ORF). Furthermore, exon 48, the exon in which mutations are most common, comprises only ~7% of the

FIG. 2. Facial photographs of mother and daughter with Kabuki syndrome in whom no causative mutation in *MLL2* was identified. Both have mild developmental delay and no known major malformations.

FIG. 3. Facial photographs of four children diagnosed with Kabuki syndrome in whom no causative mutation in *MLL2* was found. The photograph in the upper left was reprinted from Ng et al. [2010].

MLL2 ORF. Exon 39 contains several regions that encode long polyglutamine tracts suggesting the presence of a mutational hotspot, although no such explanation is obvious for exon 48. A stepwise approach in which these regions are the first screened might be a reasonable approach to diagnostic testing. However, capture of all introns, exons, and nearby *MLL2* regulatory regions followed by next-generation sequencing would be more comprehensive and likely to be less costly over the long term.

Comparison of four of the objective clinical characteristics of *MLL2* mutation-negative versus *MLL2* mutation-positive cases allowed us to explore both the relationship between *MLL2* genotype and Kabuki phenotype and the phenotype of *MLL2* mutation-negative cases. Overall, the clinical characteristics of *MLL2* mutation-positive cases did not differ significantly from *MLL2* mutation-negative cases with the exception that renal anomalies were more common in *MLL2* mutation-positive cases. Similarly, we observed no significant phenotypic—including the severity of developmental delay—differences between individuals grouped by mutation type. However, the phenotypic data available to us for analysis was limited and, for many cases, we lacked specific information about each malformation present. Furthermore, the most typical phenotypic characteristic, the distinctive facial appearance, was not compared in detail between cases although it would be of interest to study facial images "blinded" to mutation status to investigate its power to predict genotype. Analysis of genotype–phenotype relationships using both a larger set of Kabuki cases, and with access to more comprehensive phenotypic information would be valuable.

No *MLL2* mutation could be identified in 26 of the cases referred to us with a diagnosis of Kabuki syndrome. In three of these cases, aCGH identified structural variants that could be of clinical significance although additional investigation is required. A fourth case had the classical deletion observed in individuals with Sotos syndrome, and in retrospect it appears that this case was included in the cohort erroneously. The 22 remaining cases, including 1 parent-offspring pair, represent individuals with fairly classic phenotypic features of Kabuki syndrome without a *MLL2* mutation. This observation suggests that Kabuki syndrome is genetically heterogeneous. To this end, in these 22 cases, we sequenced the protein-coding exons of *UTX*, a gene that encodes a protein that directly interacts with *MLL2* but no pathogenic changes were found (data not shown). Exome sequencing of a subset of these *MLL2* mutation-negative cases to identify other candidate genes for Kabuki syndrome is underway.

Whether Kabuki syndrome is the most appropriate diagnosis for the *MLL2* mutation-negative cases is unclear. Some of the *MLL2* mutation-negative cases appear to have a facial phenotype that differs somewhat from that of the *MLL2* mutation-positive cases. Whether these *MLL2* mutation-negative cases diagnosed by expert clinicians should be considered Kabuki syndrome, a variant thereof, or a separate disorder remains to be determined. Our opinion is that there is simply not yet enough information to make an informed decision about this issue.

Most of the mutations in *MLL2* are predicted to result in haploinsufficiency. However, it is unclear by what mechanism(s) haploinsufficiency of *MLL2* could cause Kabuki syndrome. *MLL2* encodes a histone 3 lysine 4 (H3K4) methyltransferase, one of at least 10 proteins (genes for which have not to our knowledge yet been screened in Kabuki cases in which *MLL2* mutations were not found) that have been identified to specifically modify the lysine residue at the fourth amino acid position of the histone H3 protein [Kouzarides, 2007]. MLL2 has a SET domain near its C-terminus that is shared by yeast Set1, *Drosophila* Trithorax (TRX) and human MLL1 [FitzGerald and Diaz, 1999]. MLL2 appears to regulate gene transcription and chromatin structure in early development [Prasad et al., 1997]. In mice, loss of *MLL2* results in embryonic lethality before E10.5, and while $Mll2^{+/-}$ mice are viable, they are smaller than wild-type [Ng et al., 2010].

Kabuki syndrome is the most common of a small, but growing group of multiple malformation syndromes accompanied by developmental delay that are caused by mutations in genes that encode proteins involved in histone methylation [De Sario, 2009]. The most notable of these is CHARGE syndrome, which is one of the syndromes often considered in the differential diagnosis of children ultimately diagnosed with Kabuki syndrome. CHARGE syndrome is caused by mutations in *CHD7*, which encodes a chromodomain protein that recognizes the trimethylated H3K4 side chain [Vissers et al., 2004]. Other disorders caused by defects of histone methylation status include several intellectual disability syndromes, some of which are also characterized by malformations (e.g., cleft lip/palate) that overlap with those found in individuals with Kabuki syndrome.

Kabuki syndrome is one of the most common causes of heritable developmental delay. Discovery that mutations in *MLL2* are the most common cause of Kabuki syndrome highlights the role that disrupted regulation of histone methylation plays as a cause of human birth defects. Characterizing the spectrum of mutations in *MLL2* is a small but important first step toward understanding the mechanism(s) that underlies Kabuki syndrome.

ACKNOWLEDGMENTS

We thank the families for their participation and the Kabuki Syndrome Network for their support. Our work was supported in part by grants from the National Institutes of Health/National Heart Lung and Blood Institute (5R01HL094976 to D.A.N. and J.S.), the National Institutes of Health/National Human Genome Research Institute (5R21HG004749 to J.S., 1RC2HG005608 to M.J.B., D.A.N., and J.S.; and 5RO1HG004316 to H.K.T.), National Institute of Heath/National Institute of Environmental Health Sciences (HHSN273200800010C to D.N.), National Institute of Neurological Disorders and Stroke (RO1NS35102 to C.A.M.), NIHR Manchester Biomedical Research Centre (D. D.), Ministry of Health, Labour and Welfare (K.Y., N.M., T.O., and N.N.), Ministry of Health, Labour and Welfare of Japan (N.M), Japan Science and Technology Agency (N.M.), Society for the Promotion of Science (N.M.), the Life Sciences Discovery Fund (2065508 and 0905001), the Washington Research Foundation, and the National Institutes of Health/National Institute of Child Health and Human Development (1R01HD048895 to M.J.B. and 5K23HD057331 to A.E.B.). S.B.N. is supported by the Agency for Science, Technology and Research, Singapore. A.W.B. is supported by a training fellowship from the National Institutes of Health/National Human Genome Research Institute (T32HG00035).

REFERENCES

Adam MP, Hudgins L. 2005. Kabuki syndrome: A review. Clin Genet 67: 209–219.

De Sario A. 2009. Clinical and molecular overview of inherited disorders resulting from epigenomic dysregulation. Eur J Med Genet 52:363–372.

FitzGerald KT, Diaz MO. 1999. ML L2: A new mammalian member of the trx/MLL family of genes. Genomics 59:187–192.

Kouzarides T. 2007. Chromatin modifications and their function. Cell 128:693–705.

Kuroki Y, Suzuki Y, Chyo H, Hata A, Matsui I. 1981. A new malformation syndrome of long palpebral fissures, large ears, depressed nasal tip, and skeletal anomalies associated with postnatal dwarfism and mental retardation. J Pediatr 99:570–573.

Kurotaki N, Imaizumi K, Harada N, Masuno M, Kondoh T, Nagai T, Ohashi H, Naritomi K, Tsukahara M, Makita Y, Sugimoto T, Sonoda T, Hasegawa T, Chinen Y, Tomita Ha, Kinoshita HA, Mizuguchi A, Yoshiura T, Ki K, Ohta T, Kishino T, Fukushima Y, Niikawa N, Matsumoto N. 2002. Haploinsufficiency of NSD1 causes Sotos syndrome. Nat Genet 30:365–366.

Ng SB, Bigham AW, Buckingham KJ, Hannibal MC, McMillin MJ, Gildersleeve HI, Beck AE, Tabor HK, Cooper GM, Mefford HC, Lee C, Turner EH, Smith JD, Rieder MJ, Yoshiura K, Matsumoto N, Ohta T, Niikawa N, Nickerson DA, Bamshad MJ, Shendure J. 2010. Exome sequencing identifies MLL2 mutations as a cause of Kabuki syndrome. Nat Genet 42:790–793.

Niikawa N, Matsuura N, Fukushima Y, Ohsawa T, Kajii T. 1981. Kabuki make-up syndrome: A syndrome of mental retardation, unusual facies, large and protruding ears, and postnatal growth deficiency. J Pediatr 99:565–569.

Niikawa N, Kuroki Y, Kajii T, Matsuura N, Ishikiriyama S, Tonoki H, Ishikawa N, Yamada Y, Fujita M, Umemoto H, et al. 1988. Kabuki make-up (Niikawa-Kuroki) syndrome: A study of 62 patients. Am J Med Genet 31:565–589.

Prasad R, Zhadanov AB, Sedkov Y, Bullrich F, Druck T, Rallapalli R, Yano T, Alder H, Croce CM, Huebner K, Mazo A, Canaani E. 1997. Structure and expression pattern of human ALR, a novel gene with strong homology to ALL-1 involved in acute leukemia and to Drosophila trithorax. Oncogene 15:549–560.

Vissers LE, van Ravenswaaij CM, Admiraal R, Hurst JA, de Vries BB, Janssen IM, van der Vliet WA, Huys EH, de Jong PJ, Hamel BC, Schoenmakers EF, Brunner HG, Veltman JA, van Kessel AG. 2004. Mutations in a new member of the chromodomain gene family cause CHARGE syndrome. Nat Genet 36:955–957.

White SM, Thompson EM, Kidd A, Savarirayan R, Turner A, Amor D, Delatycki MB, Fahey M, Baxendale A, White S, Haan E, Gibson K, Halliday JL, Bankier A. 2004. Growth, behavior, and clinical findings in 27 patients with Kabuki (Niikawa-Kuroki) syndrome. Am J Med Genet Part A 127A:118–127.

REPORT

Mutations in *POLR3A* and *POLR3B* Encoding RNA Polymerase III Subunits Cause an Autosomal-Recessive Hypomyelinating Leukoencephalopathy

Hirotomo Saitsu,[1,*] Hitoshi Osaka,[2] Masayuki Sasaki,[3] Jun-ichi Takanashi,[4] Keisuke Hamada,[5] Akio Yamashita,[6] Hidehiro Shibayama,[7] Masaaki Shiina,[5] Yukiko Kondo,[1] Kiyomi Nishiyama,[1] Yoshinori Tsurusaki,[1] Noriko Miyake,[1] Hiroshi Doi,[1] Kazuhiro Ogata,[5] Ken Inoue,[8] and Naomichi Matsumoto[1,*]

Congenital hypomyelinating disorders are a heterogeneous group of inherited leukoencephalopathies characterized by abnormal myelin formation. We have recently reported a hypomyelinating syndrome characterized by diffuse cerebral hypomyelination with cerebellar atrophy and hypoplasia of the corpus callosum (HCAHC). We performed whole-exome sequencing of three unrelated individuals with HCAHC and identified compound heterozygous mutations in *POLR3B* in two individuals. The mutations include a nonsense mutation, a splice-site mutation, and two missense mutations at evolutionally conserved amino acids. Using reverse transcription-PCR and sequencing, we demonstrated that the splice-site mutation caused deletion of exon 18 from *POLR3B* mRNA and that the transcript harboring the nonsense mutation underwent nonsense-mediated mRNA decay. We also identified compound heterozygous missense mutations in *POLR3A* in the remaining individual. *POLR3A* and *POLR3B* encode the largest and second largest subunits of RNA Polymerase III (Pol III), RPC1 and RPC2, respectively. RPC1 and RPC2 together form the active center of the polymerase and contribute to the catalytic activity of the polymerase. Pol III is involved in the transcription of small noncoding RNAs, such as 5S ribosomal RNA and all transfer RNAs (tRNA). We hypothesize that perturbation of Pol III target transcription, especially of tRNAs, could be a common pathological mechanism underlying *POLR3A* and *POLR3B* mutations.

Congenital hypomyelinating disorders form a heterogeneous group of central nervous system leukoencephalopathies that is characterized by abnormal myelin formation. Although these conditions are readily recognized by brain magnetic resonance imaging (MRI), many cases are not diagnosed correctly.[1] Several syndromes affecting myelination, such as hypomyelination with hypodontia and hypogonadotropic hypogonadism (4H) syndrome (MIM 612440) and hypomyelination with atrophy of the basal ganglia and cerebellum (H-ABC) (MIM 612438), have been described.[2–5] We have recently reported a hypomyelinating syndrome characterized by diffuse cerebral hypomyelination with cerebellar atrophy and hypoplasia of the corpus callosum (HCAHC).[6] Individuals with HCAHC do not show hypodontia or atrophy of the basal ganglia, which are observed in 4H syndrome and H-ABC; however, diffuse hypomyelination, atrophy, or hypoplasia of the cerebellum and corpus callosum are overlapping features of these three syndromes, suggesting that there might be a common underlying pathological mechanism.

Here, we report on four individuals with HCAHC from three unrelated families (Figure 1A; Table 1). Clinical information and peripheral blood or saliva samples were obtained from the family members after obtaining written informed consent. Experimental protocols were approved by the Institutional Review Board of Yokohama City University. To identify pathogenic mutations, we performed whole-exome sequencing of three probands from three unrelated families (individuals 1, 3, and 4). DNAs were captured with the SureSelect Human All Exon 50Mb Kit (Agilent Technologies, Santa Clara, CA) and sequenced with one lane per sample on an Illumina GAIIx (Illumina, San Diego, CA) with 108 bp paired-end reads. Image analysis and base calling were performed by sequence control software real-time analysis and CASAVA software v1.7 (Illumina). A total of 90,014,368 (individual 1), 86,942,264 (individual 3), and 92,168,758 (individual 4) paired-end reads were obtained and aligned to the human reference genome sequence (GRCh37/hg19) with MAQ[7] and NextGENe software v2.00 with sequence condensation by consolidation (SoftGenetics, State College, PA). This approach resulted in more than 88% of target exomes being covered by ten reads or more (see Table S1, available online). Single nucleotide variants (SNVs) were called with MAQ and NextGENe. Small insertions and deletions were

[1]Department of Human Genetics, Yokohama City University Graduate School of Medicine, 3-9 Fukuura, Kanazawa-ku, Yokohama 236-0004, Japan; [2]Division of Neurology, Clinical Research Institute, Kanagawa Children's Medical Center, 2-138-4 Mutsukawa, Minami-ku, Yokohama 232-8555, Japan; [3]Department of Child Neurology, National Center of Neurology and Psychiatry, 4-1-1 Ogawahigashi-cho Kodaira, Tokyo 187-8551, Japan; [4]Department of Pediatrics, Kameda Medical Center, 929 Higashi-cho, Kamogawa-shi, Chiba 296-8602, Japan; [5]Department of Biochemistry, Yokohama City University Graduate School of Medicine, 3-9 Fukuura, Kanazawa-ku, Yokohama 236-0004, Japan; [6]Department of Molecular Biology, Yokohama City University Graduate School of Medicine, 3-9 Fukuura, Kanazawa-ku, Yokohama 236-0004, Japan; [7]Department of Neurology, Kameda Medical Center, 929 Higashi-cho, Kamogawa-shi, Chiba 296-8602, Japan; [8]Department of Mental Retardation and Birth Defect Research, National Institute of Neuroscience, National Center of Neurology and Psychiatry, 4-1-1 Ogawahigashi-cho Kodaira, Tokyo 187-8551, Japan
*Correspondence: hsaitsu@yokohama-cu.ac.jp (H.S.), naomat@yokohama-cu.ac.jp (N.M.)
DOI 10.1016/j.ajhg.2011.10.003.

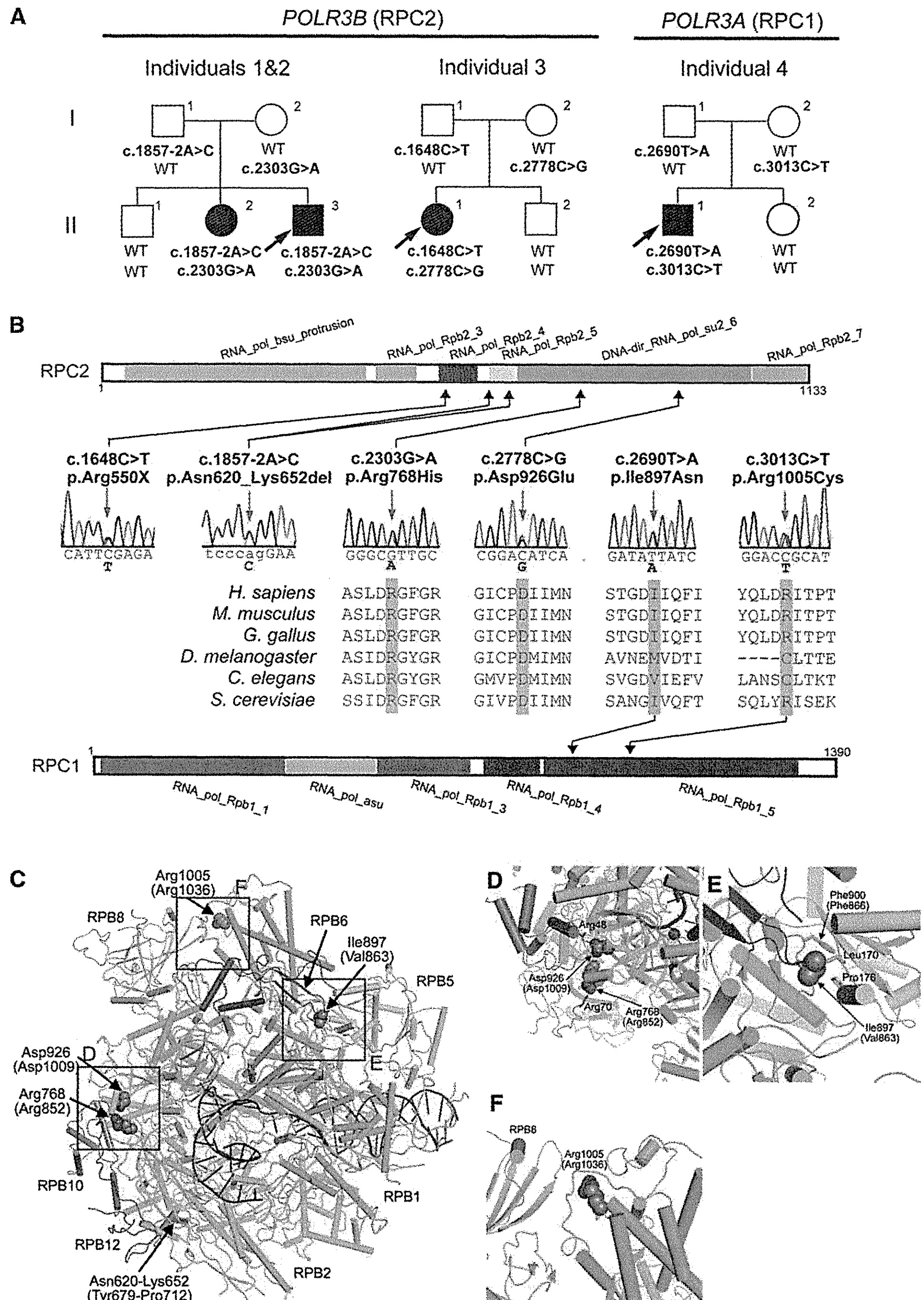

Figure 1. Mutations in *POLR3B* and *POLR3A*

(A) Pedigrees of four kindreds with HCAHC are shown. We identified four mutations in *POLR3B* encoding RPC2 in three individuals from two unrelated families and two mutations in *POLR3A* encoding RPC1 in one family. The segregation of each mutation is shown.

(B) Schematic representation of RPC2 (upper) and RPC1 (lower) proteins with Pfam domains (from Ensembl). Locations of each amino-acid-altering mutation are depicted with electropherograms. All of the missense mutations occurred at evolutionally conserved amino acids. Homologous sequences were aligned with the CLUSTALW website.

(C–F) 3D representations of RPC1 and RPC2 mutations. Mutated amino acids in RPC1 and RPC2 are shown along with their equivalent positions in the homologous RPB1 and RPB2 subunits of RNA Polymerase II (amino acid and its position in parenthesis). The structure and positions of mutations are illustrated by PyMOL with the crystal structure (PDB accession number 3GTP). RPB3, RPB9, and RPB11 subunits, which are specific to RNA Polymerase II, have been omitted from the figure. RPB1 is shown in green, RPB2 in sky blue, RPB5 in yellow, RPB6 in dark blue, RPB8 in pink, RPB10 in orange, RPB12 in purple, DNA in brown, and RNA in red. Amino acids that interact with mutated amino acids are also shown.

Table 1. Clinical Features of the Individuals

Clinical Features	Individual 1	Individual 2	Individual 3	Individual 4
Genes	*POLR3B*	*POLR3B*	*POLR3B*	*POLR3A*
Mutations, DNA	c.1857-2A>C, c.2303G>A	c.1857-2A>C, c.2303G>A	c.1648C>T, c.2778C>G	c.2690T>A, c.3013C>T
Mutations, protein	p.Asn620_Lys652del, p.Arg768His	p.Asn620_Lys652del, p.Arg768His	p.Arg550X, p.Asp926Glu	p.Ile897Asn, p.Arg1005Cys
Gender	M	F	F	M
Current age (years)	27	30	16	17
Intellectual disability	mild	mild	moderate	mild
Cognitive regression	–	–	–	–
Seizures	–	–	–	–
Initial motor development	normal	normal	normal	normal
Age of onset (years)	3	3	2	4
Motor deterioration	–	–	–	+
Wheelchair use	–	–	–	+
Optic atrophy	–	–	–	–
Myopia	+	+	–	+
Nystagmus	+	+	–	–
Abnormal pursuit	+	+	+	–
Vertical gaze limitation	+	+	+	–
Dysphagia	–	–	+	–
Hypersalivation	–	–	–	–
Cerebellar signs	+	+	+	+
Tremor	–	+	+	+
Babinski refex	–	–	–	–
Spasticity	–	–	mild	–
Peripheral nerve involvement	–	–	–	–
Nerve biopsy	NA	NA	NA	NA
Hypodontia	–	–	–	–
Hypogonadism	+	+	–	–

NA is an abbreviation for not available.

detected with NextGENe. Called SNVs were annotated with SeattleSeq Annotation.

We adopted a prioritization scheme to identify the pathogenic mutation in each individual, similar to the approach taken by recent studies (Table S2).[8–10] First, we excluded the variants registered in the dbSNP131 or 1000 Genome Project from all the detected variants. Then, SNVs commonly detected by MAQ and NextGENe analyses were selected as highly confident variants; 364 to 374 SNVs of nonsynonymous (NS) or canonical splice-site (SP) changes, along with 113 to 124 small insertions or deletions (indels), were identified per individual. We also excluded variants found in our 55 in-house exomes, which are derived from 12 healthy individuals and 43 individuals with unrelated diseases, reducing the number of candidate variants to ~250 per individual. Assuming that HCAHC is an autosomal-recessive disorder based on two affected individuals in one pedigree (individuals 1 and 2), we focused on rare heterozygous variants that are not registered in the dbSNP or in our in-house 55 exomes.

We surveyed all genes in each individual for two or more NS, SP, or indel variants. We found three to eight candidate genes per individual (Table S2). Among them, only *POLR3B* encoding RPC2, the second largest subunit of RNA Polymerase III (Pol III), was common in two individuals (individuals 1 and 3). The inheritance of the variants in *POLR3B* (transcript variant 1, NM_018082.5) was examined by Sanger sequencing. In individual 1, we confirmed that a canonical splice-site mutation (c.1857-2A>C [p.Asn620_Lys652del]), 2 bp upstream of exon 18, was